Philosophical Magazine Letters,
Vol. 86, No. 10, October 2006, 651–659

Taylor & Francis
Taylor & Francis Group

Negative incremental bulk modulus in foams

B. MOORE†, T. JAGLINSKI‡, D. S. STONE†‡ and R. S. LAKES*‡§¶

†Department of Materials Science and Engineering, University of Wisconsin-Madison, Madison, WI 53706-1687, USA
‡Materials Science Program, University of Wisconsin-Madison, Madison, WI 53706-1687, USA
§Department of Engineering Physics, University of Wisconsin-Madison, Madison, WI 53706-1687, USA
¶Biomedical Engineering Department and Rheology Research Center, University of Wisconsin-Madison, 147 Engineering Research Building, 1500 Engineering Drive, Madison, WI 53706-1687, USA

(*Received 3 April 2006; in final form 9 August 2006*)

Negative incremental stiffness is known to occur in structures such as post-buckled flexible tubes and single-cell models. A single foam cell under uniaxial loading buckles and exhibits a non-monotonic S-shaped deformation curve, which is indicative of negative incremental stiffness. Negative stiffness is not observed in bulk materials. For example, individual foam cells display negative stiffness but foams tested in uniaxial compression exhibit a plateau in the stress–strain curve because the buckled cells localize in bands. This behaviour is consistent with the continuum view in which strong ellipticity and, hence, a positive shear modulus G and positive C_{11} modulus are required for stability, even for a constrained object. It is hypothesized that a solid with negative bulk modulus can be stabilized by control of the surface displacement. Experimentally, foams were hydrostatically compressed by controlled injections of small volumes of water into a plastic chamber, causing volumetric deformation. A negative incremental bulk modulus was observed in a foam with 0.4-mm cell size beyond about 20% volumetric strain. A foam with large cells, 2.5–4 mm in size, was anisotropic and did not exhibit the cell buckling required for negative modulus.

1. Introduction

Negative stiffness, or a reversal in the usual assumed direction between a force and the resulting deformation, is known to occur in buckled structural elements [1]. It is distinct from a negative Poisson's ratio [2], which is a reversal of the usual relation between transverse and longitudinal strains observed in tension or compression. If the slope of the force–deformation curve is negative at zero force, it represents a negative stiffness. If the slope becomes negative at a non-zero load, the curve is non-monotonic and the negative slope represents a negative incremental stiffness. Negative incremental stiffness is observed experimentally provided the unstable structural element undergoing buckling is constrained. Stable, negative incremental

*Corresponding author. Email: lakes@engr.wisc.edu

Philosophical Magazine Letters
ISSN 0950-0839 print/ISSN 1362-3036 online © 2006 Taylor & Francis
http://www.tandf.co.uk/journals
DOI: 10.1080/09500830600957340

stiffness has been demonstrated for post-buckled rubber tubes constrained in displacement control [3]. In displacement control, the displacement of the test machine actuator is prescribed and the load measured, preventing the catastrophic failure normally observed during buckling as progressively larger loads are applied. Similarly, Rosakis *et al.* [4] demonstrated non-monotonic behaviour in load deformation curves for a constrained model of a single foam cell, indicative of incremental negative stiffness, as shown in figure 1. The effect is due to buckling of the cell ribs. Also shown in figure 1 is the monotonic behaviour of foam material containing many such cells. The buckled cells in the foam are under insufficient constraint; they localize to form bands transverse to the applied compression.

The negative stiffness concept has also been theoretically analyzed and experimentally studied in composite materials. Such composites can exhibit material properties that exceed conventional bounds on composite material behaviour; formulae describing such behaviour tacitly assume positive moduli in their derivation [5]. For example, in a lumped system consisting of single post-buckled rubber tubes in series with elastic elements, an increase over the base material in viscoelastic damping by orders of magnitude was observed [3].

For the case of distributed systems (i.e. bulk materials), negative moduli can be achieved through ferroelastic [6], and martensitic [7] transformations. These transformations are rapid, diffusionless crystal structure rearrangements that can be induced through temperature changes and mechanical stress [8]. Negative moduli arise in these reactions within the context of Landau theory [9] from the formation of two local minima in the strain energy function. As the temperature is lowered, an energy function with a single minimum, representing the equilibrium high-temperature phase, gradually flattens, then develops two minima. Since the curvature of this energy profile represents a modulus, the flattening of the curve corresponds to

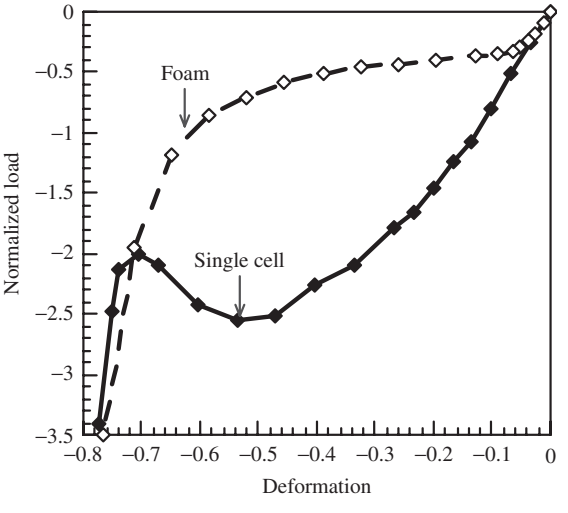

Figure 1. Comparison of observed behaviour of a single cell model displaying non-monotonic, negative stiffness behaviour and of a foam made of such cells, both under displacement control, adapted from Rosakis *et al.* [4].

a softening of the modulus toward zero at the critical temperature T_c. Below T_c, the relative maximum and, hence, negative curvature between the two potential wells represents a negative modulus. This condition is unstable, and bands of material form, visible as the twin structures associated with ferroelastic and martensitic reactions, with strains of opposite sign corresponding to the new relative minima.

Negative stiffness or the modulus of an unconstrained object entails instability and is not normally observed or measured. However, if the displacement is constrained, an object with negative structural stiffness (or spring constant) can be stable. From a continuum standpoint, to achieve a negative elastic modulus surface constraint is necessary but is not sufficient for stability. For example, an isotropic solid under rigid constraint is stable provided it is strongly elliptic, which allows a range of from $-\infty$ to ∞ for Young's modulus E and $-4G/3$ to ∞ for the bulk modulus B, with the shear modulus $G > 0$ [10]. For ferroelastic and martensitic materials in the vicinity of a phase transformation, the shear modulus G can soften to zero. Below the transformation temperature, the material develops bands or domains due to the instability and the stiffness remains positive. For example, in single crystals of indium–thallium alloys, which undergo a martensitic transformation, a shear modulus tends to zero, but does not go negative [11, 12]. This is not surprising since these crystals are not constrained on all surfaces.

To achieve a negative modulus, the banding instability associated with failure of strong ellipticity may be suppressed by surface effects. In particular, sufficiently small single crystals can be single domain. The reason is that the energy required to form domain boundaries is dominated by crystal surface energy. Single-domain crystals are predicted to exhibit negative shear modulus under constraint. Composites with spherical negative stiffness inclusions [5] may be stable provided the stiffness of the inclusion is not too negative. Metal matrix composites [13], with ferroelastic vanadium dioxide as the phase-transforming negative-stiffness inclusions, were fabricated and studied; they exhibited gigantic peaks in mechanical damping and anomalies in the modulus, in harmony with theoretical predictions [14]. In these results, a negative inclusion shear modulus was inferred but not measured directly.

Stable, negative elastic moduli have not been measured directly on any material. The effects of negative incremental structural stiffness in foam cells are illustrated in figure 1. In this experiment, the negative structural stiffness, indicated by the negative slope in the load–deformation plot of the single cell, was stabilized by a constraint on the displacement. By contrast, a material made of many of such cells exhibits a monotonic load–deformation plot with positive stiffness throughout. Buckling of the individual cells gives rise to bands of localized heterogeneous deformation in the foam resulting in the plateau region beyond about 5% deformation strain in compression. In the continuum view, loss of local stability corresponds to the destabilizing effect of a negative value of the compression modulus C_{11}. The continuum view described above suggests that a material possessing a negative bulk modulus B could be stabilized by a surface constraint. In the present work, a negative incremental bulk modulus is demonstrated experimentally in pre-strained foam under control of the volumetric deformation.

2. Experiment

2.1. *Materials*

Open cell foams were obtained from Foamade Industries (Auburn Hills, MI, USA) and from Foamex International (Eddystone, PA, USA). These foams had pore sizes of 2.5 mm (10 pores per inch (ppi)) and 0.4 mm (60 ppi). Cubes, cylinders and spheres were cut from the bulk foam via an iterative sectioning process; portions of foam were sectioned and the specimen measured. Any irregularities were further sectioned. Specimens included cubes with side lengths of about 2.5 cm, cylinders that were about 3 cm in diameter and 4.5 cm long, and spheres about 3.5 cm in diameter.

2.2. *Uniaxial compression*

Specimens were tested in uniaxial compression to obtain Young's modulus, to determine the degree of anisotropy and obtain a uniaxial deformation curve to compare with that of volumetric deformation. A MTS screw-driven test machine with a 45-N (10 lb) load cell was used. Specimens were tested at various deformation rates.

2.3. *Volumetric compression*

Foam specimens were sealed inside a cylindrical natural latex rubber membrane 0.076 mm thick (Trojan, Church & Dwight Co., Princeton, NJ, USA). Initial trials were conducted with cubic specimens enclosed in flat latex membranes 0.15 mm thick (McMaster-Carr, Chicago, IL, USA) cemented together in segments. However, an adequate seal under water compression was difficult to maintain, so cylindrical membranes were used. After first inserting the specimen all the way to the end of the membrane, a 3-mm diameter air relief tube was then placed into the membrane (figure 2). The membrane was then twisted around the tube to take up the slack and remove as much air as possible without placing a pre-compression on the specimen. Several windings of electrical tape were then tightly wrapped around the tube and membrane. After sealing, the excess latex was trimmed and removed.

A volumetric test chamber was fabricated from a 1–l polycarbonate bottle (Nalgene, Rochester, NY, USA). The screw top was modified by first drilling a hole through the cap and adding a bulkhead joint to allow the air relief tube to feed through and supply a water injection port (figure 2). Known volumes of water were injected by a calibrated screw piston. Gauge pressure was measured using a digital HHP-2021 manometer (Omega) with a 13-kPa operating range; the manometer requires an input tube of 4 mm inner diameter and 1 mm wall thickness. The manometer is only capable of reading air pressure so the last section of the manometer tube, roughly 10 cm, was left unfilled with water. Owing to the high bulk modulus of the water (about 2 GPa), in comparison to the foam ($\sim$50 kPa), and the high structural stiffness and small volume of the bottle, this experimental setup corresponds to a nearly perfect, displacement-controlled test machine.

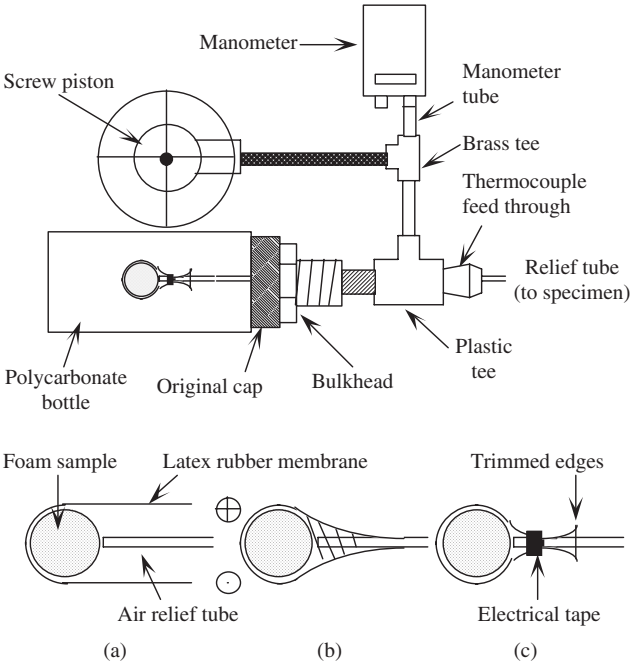

Figure 2. Top view of the test chamber, a manometer to measure pressure and a piston plunger to impose a volume change. The detail below shows the specimen set-up procedure. (a) Insertion of specimen membrane with air escape tube, (b) twisting of membrane around relief tube until slack is taken up, and (c) sealing of specimen with several windings of electrical tape.

Tests were set up by first filling the chamber with tap water and placing the lid tightly onto the chamber. The thermocouple feed through was unscrewed and the chamber was topped off with water through this opening. Once the water level reached the thermocouple feed-through hole, the fitting was replaced and the chamber turned upside down and slightly agitated to release any remaining air bubbles. The chamber was then returned upright, the thermocouple feed-through removed and water was added as needed. This process was repeated until all the visible air bubbles were bled from the system. Once the system was free of bubbles, the manometer was attached and the initial pressure reading recorded.

Volumetric compression was initiated by incrementally backing off on the volume until the membrane was observed visually to be inflated beyond the diameter of the sample. Water was then displaced into the system in small increments of about 0.14 ml. After each displacement increment, the manometer was allowed to settle to a constant pressure. A typical compression test to 40% strain took typically up to 5 h. A zero strain point was inferred based on the slope change during the ballooning of the latex rubber.

After compression testing, each specimen was completely removed from the pressure chamber, unwrapped and allowed to recover for at least 10 times the duration of the test. For consecutive tests the specimen was wrapped in a new membrane for each test.

3. Results

Uniaxial compression of the various foams (figure 3) was indicative of classic foam behaviour, showing an initial seating effect, then a linearly elastic region of 5–10% strain, a plateau region and finally densification after about 70% strain (figure 4). Strains were calculated simply from the actuator motion. For foams of small pore size, Young's modulus was of the order of 50 kPa and was sensitive to direction. In figure 4, the Young's moduli of the 25.4-mm Foamade cube were 47, 34 and 37 kPa for directions 1, 2 and 3, respectively, thus yielding anisotropy ratios of 1.0:1.1:1.4. Similarly, the 25.4-mm Foamex cube returned moduli of 31, 31 and 47.5 kPa, or ratios of 1.0:1.0:1.5. The larger cell foams showed a more pronounced directional dependence owing to the elongated pore shape, and moduli of 9, 9 and

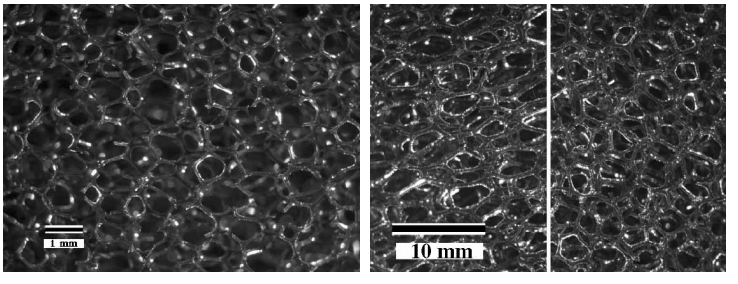

Figure 3. Foam structure. (a) Foamade and Foamex foams, cell size 0.4 mm; scale bar is 1 mm. (b) Foamex foam of 0.8 mm cell size showing elongated pore shape in one direction (left); scale bar is 10 mm.

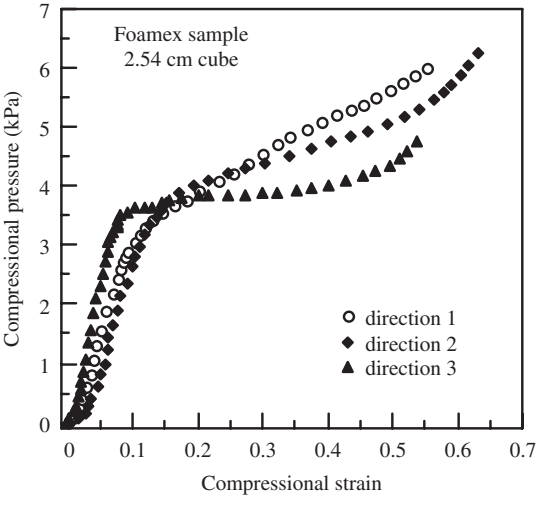

Figure 4. Uniaxial compression stress–strain curves from a Foamex 25.4 mm cube (0.4 mm cell size) displaying classic foam behaviour. Some directional dependence is evident, with Young's moduli of 34, 37 and 47 kPa for directions 1, 2 and 3, respectively.

20 kPa with the 25.4-mm sample, or ratios of 1.0:1.0:2.2. In contrast, a 50.8-mm cube of the same foam had moduli of 15, 15 and 37.5 kPa, or 1.0:1.0:2.5.

Volumetric compression experiments disclosed non-monotonic behaviour provided the foam specimen had small cells (0.4 mm) and was spherical in shape (figure 5). Beyond about 20% strain, the incremental bulk modulus became negative. Cycle dependence was observed in which the initial foam modulus decreased and the large-strain behaviour changed character. Figure 5 shows behaviour of 0.4 mm cell size Scott Industrial foam [15] cut from a previously tested foam cylinder, and figure 6 shows similar non-monotonic behaviour of a spherical specimen having a similar 0.4-mm cell size, recently obtained from Foamex Industries.

In contrast, cylinders made from the 2.5-mm cell (10 ppi) foams, subjected to hydrostatic compression, displayed behaviour that was dominated by anisotropy. Specimen deformation was heterogeneous; the cylinders deformed into an hourglass shape at high strains. Cylinders made from the smaller cell size foams also displayed heterogeneous deformation, most likely due to the intrinsic shape of the rubber membrane. Non-monotonic behaviour was not observed in these tests. Typical response curves are shown in figure 7.

4. Discussion

Negative bulk modulus was observed in the hydrostatic compression of small cell (0.4 mm) foam under control of volumetric displacement, for deformations of 20–35%. This is, therefore, an incremental bulk modulus. The effect is attributed to buckling of the cell ribs. In the continuum view, a material with a negative bulk modulus can be stabilized by a constraint, but a negative shear modulus or

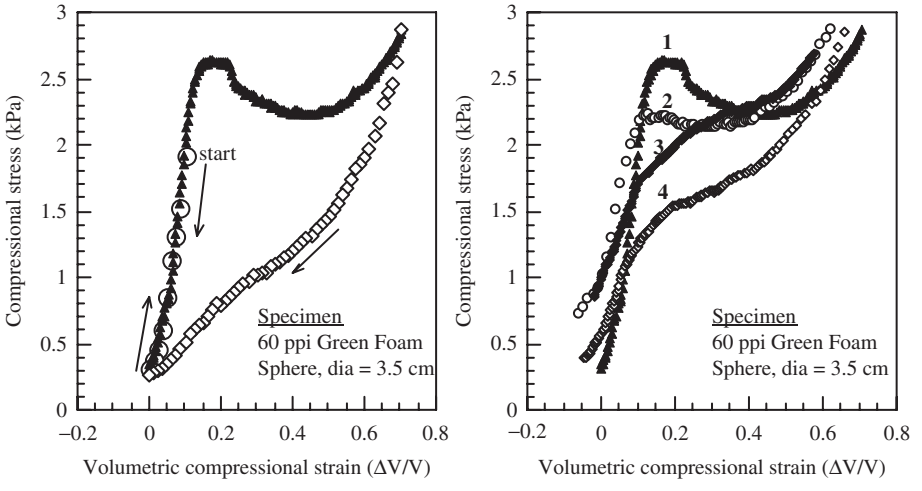

Figure 5. (a) Hydrostatic compression hysteresis and non-monotonic behaviour in a load–unload cycle of a 60-ppi, 3.5-cm diameter sphere in displacement (volumetric) control. (b) Cycle dependence in repeated tests 1, 2, 3 and 4.

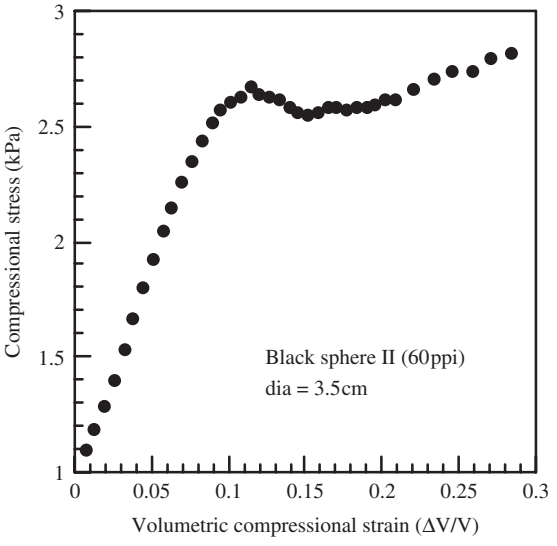

Figure 6. Non-monotonic behaviour in a sphere of 0.4 mm cell size Foamex foam.

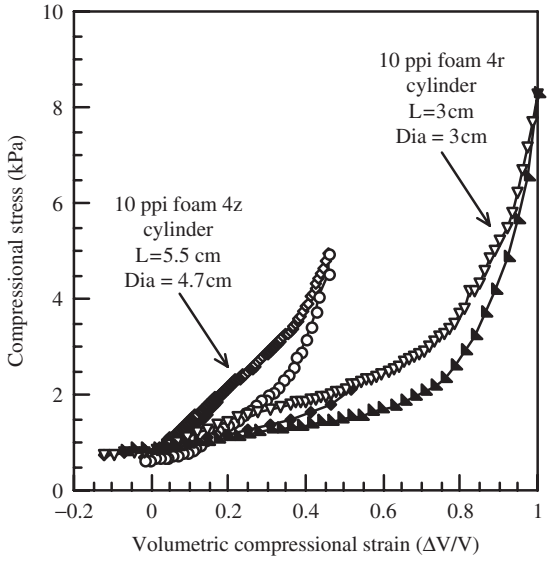

Figure 7. Hydrostatic compression response curves for loading and unloading of 2.5 mm cell (10 ppi) foam cylinders with long direction of pores oriented with the cylinder's long direction (4z) and aligned perpendicular to the long axis of the cylinder (4r).

C_{11} modulus is unstable even under constraint. The large cell (2.5 mm) foam exhibited monotonic load–deformation curves with positive bulk modulus throughout. For these foams, both anisotropic cells and substantial anisotropic deformation were observed. Non-monotonic behaviour was suppressed through cell flattening,

which gave rise to bending rather than buckling of the ribs. Symmetric buckling of the cell ribs appears to be necessary for negative bulk modulus.

The hysteresis observed in load–unload cycles was larger in small cell (0.4 mm) foam than in large cell (2.5 mm) foam. It is likely that the more symmetric compression of the small cell foam gave rise to higher local strain in the cell ribs and, hence, more hysteresis. This could account for the cycle dependence observed in these materials.

5. Conclusions

Negative incremental bulk modulus was directly observed in foam with 0.4 mm cell size beyond about 20% volumetric strain. It is believed that this is the first report of a stable negative modulus (in contrast to a structural stiffness). Large cell (2.5 mm) foam exhibited anisotropic deformation under hydrostatic loading and did not exhibit a negative modulus.

Acknowledgment

The authors are grateful for a grant, CMS-9896284, from NSF.

References

[1] J.M.T. Thompson, Phil. Trans. R. Soc. Lond. **292** 1 (1979).
[2] R.S. Lakes, Science **235** 1038 (1987).
[3] R.S. Lakes, Phil. Mag. Lett. **81** 95 (2001).
[4] P. Rosakis, A. Ruina and R.S. Lakes, J. Mater. Sci. **28** 4667 (1993).
[5] R.S. Lakes and W.J. Drugan, J. Mech. Phys. Solids **50** 979 (2002).
[6] E.K.H. Salje, *Phase Transformations in Ferroelastic and Co-elastic Crystals*, Chapter 1 (Cambridge University Press, Cambridge, 1990), p. 5.
[7] T. Jaglinski, P. Frascone, B. Moore, *et al*., Phil. Mag. **86** 4285 (2006).
[8] E.K.H. Salje, *Phase Transformations in Ferroelastic and Co-elastic Crystals*, Chapter 2 (Cambridge University Press, Cambridge, 1990), p. 9.
[9] F. Falk, Acta Metall. **28** 1773 (1980).
[10] J.K. Knowles and E. Sternberg, J. Elast. **8** 329 (1978).
[11] N.G. Pace and G.A. Saunders, Proc. R. Soc. Lond. A **326** 521 (1972).
[12] D.J. Gunton and G.A. Saunders, Solid State Commun. **14** 865 (1974).
[13] R.S. Lakes, T. Lee, A. Bersie, *et al*., Nature **410** 565 (2001).
[14] R.S. Lakes, Phys. Rev. Lett. **86** 2897 (2001).
[15] B. Brandel and R.S. Lakes, J. Mater. Sci. **36** 5885 (2001).